Energy Proceedings
Vol 36, 2023
ISSN 2004-2965

Multi-objective co-optimization of networked fuel cell hybrid vehicle considering signal light information

Liang Chang[12], Baodi Zhang[12*]

1 School of Mechanical, Electronic and Control Engineering, Beijing Jiaotong University, Beijing, 100044, China

2 Beijing Key Laboratory of Powertrain Technology for New Energy Vehicles, Beijing 100044,China
(*Corresponding Author: zhangbd@bjtu.edu.cn)

ABSTRACT

In urban driving scenarios, fuel cell hybrid vehicle (FCHV) needs to face mixed driving scenarios while taking into account multiple objectives such as traffic safety, driving comfort and energy efficiency. The trade-off problem of multi-objective co-optimization is ignored for cruise control and energy management strategy (EMS), which are easily affected by the predefined driving cycle constraints. In this paper, the integrated control framework of cooperative adaptive cruise control (CACC) and EMS is established, and the chaotic multi-objective particle swarm optimization algorithm (CMOPSO) is adopted to optimize the control parameters of the integrated framework. The results show that compared with the control strategy optimized based on WLTC conditions, it can reduce the integrated energy consumption (4.1%) and the following safety (58.1%) while meeting the driving comfort requirements. Compared with the weighted sum method, the proposed method can achieve the balance of multiple optimization objectives.

Keywords: fuel cell, networked vehicle, multi-objective optimization, cooperative adaptive cruise control

NONMENCLATURE

Abbreviations

CACC	Cooperative adaptive cruise control
CMOPSO	Chaos multi-objective PSO
EMS	Energy management strategy
FCEV	Fuel cell electric vehicle
ITS	Intelligent transportation system
SOC	State-of-charge
V2I	Vehicle to infrastructure
V2V	Vehicle to vehicle
WLTC	Worldwide harmonized light vehicles test cycle

1. INTRODUCTION

Fuel cell hybrid vehicle (FCHV), with the advantages of zero emission and high energy conversion efficiency, are considered as one of the main technological ways to achieve carbon reduction in the transportation industry [1]. Currently, attention has been devoted to the research of energy management strategies (EMS) for FCHV to achieve the improvement of vehicle performance by reasonably coordinating the power allocation among multiple power sources [2], in which the standard driving cycle is used as a predefined constraint for performance optimization [3]. The optimized EMS is less adaptive and susceptible to disturbances from external driving conditions, leading to a decrease in overall vehicle economy and durability [4]. Therefore, co-optimization of longitudinal and powertrain control is needed.

Intelligent Transportation Systems (ITS) can be used to further exploit vehicle performance [5], with internet-connected vehicles sensing road information through connected vehicle technologies. Meanwhile, the longitudinal driving of vehicles is gradually shifting to automatic control, which includes cooperative adaptive cruise control (CACC) with extended communication capabilities [6]. Therefore, FCHV can improve driving safety and fuel economy through the cooperative optimization of EMS and CACC. However, the complex driving scenarios bring optimization challenges, one is the external longitudinal control. The second is the energy distribution of powertrain [7]. Therefore, existing integrated control schemes are usually designed as two layers [8]. The integration of cruise control and EMS can improve the performance of the vehicle, but it also brings complex optimization problems.

However, most research have focused on limited driving scenarios. Therefore, research on vehicle optimization in signal light scenarios was started , and the

This is a paper for the 9th Applied Energy Symposium: Low Carbon Cities and Urban Energy Systems (CUE2023), Sep. 2-7, 2023, Matsue & Tokyo, Japan.

longitudinal control was extended by considering the safety of vehicle driving [9]. Reference [10] divided urban roads into cruising zones and signal-induced zones, and judged whether a vehicle could pass through a signalized intersection by predicting its behavior. From the perspective of objective function, most of the existing methods set different weighting factors to transform the multi-objective problem into a single-objective problem. However, the multi-objectives interact with each other, and it is easy to mislead the optimization results by setting weighting coefficients artificially. The Pareto-based optimization method can balance the multi-objective problem well, but the co-optimization of the control parameters of the CACC and EMS integrated framework for FCHV in driving scenarios has not yet been studied.

Based on the above discussion, this paper co-optimizes the CACC and EMS of FCHV to balance driving safety, comfort, economy and power durability. Considering the complexity of the actual driving scenarios, acceleration control models under the scenarios of following, free cruise and signal guidance are established. Meanwhile, in order to avoid the imbalance of optimization results caused by improper multi-objective weight setting, Pareto-based chaotic multi-objective particle swarm optimization (CMOPSO) is adopted to find the optimal parameters of the integration framework.

2. MODELLING OF VEHICLE POWERTRAIN

The powertrain of FCHV is shown in Fig.1. The powertrain consists of fuel cell, power cell, electric motor etc. The parameters of the whole vehicle are shown in Table 1.

Table 1 Main parameters of vehicle

Components	Parameters	Value
Vehicle	Curb weight (kg)	2480
	Windward area (m^2)	2.204
	Rolling resistance coefficient (-)	0.01
	Drag coefficient (-)	0.29
	Wheel radius (m)	0.324
	Gear ratio (-)	8.28
Fuel Cell	Rated power (kW)	36
	Peak power (kW)	38
	Number of series cells	174
Battery	Capacity (Ah)	37
	Peak power (kW)	70

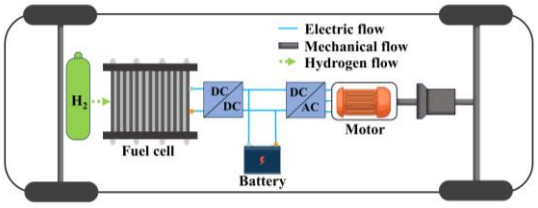

Fig. 1. Powertrain architecture of FCHV

2.1 Fuel cell model

The fuel cell model is recognized based on the experimental data of fuel cell output characteristics. The results of the comparison between the simulated and experimental values of the identified model are shown in Fig. 2.

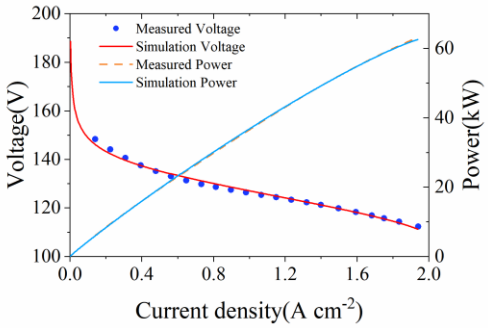

Fig. 2. Simulation of fuel cell stack polarization curve

2.2 Battery model

The power battery model takes the equivalent internal resistance model, and the power battery current expression is:

$$I_b = \frac{V_{oc} - \sqrt{V_{oc}^2 - 4R_{bat}P_{bat}}}{2R_{bat}} \quad (1)$$

Where: I_b is the power cell current (A), V_{OC} is the power cell open-circuit voltage (V), R_{bat} is the equivalent internal resistance of the power cell (Ω), P_{bat} is the power of the power cell (kW).

The current state-of-charge (SOC) of the battery, expressed as:

$$SOC = SOC_{t_0} - \frac{1}{Q_b}\int_{t_0}^{t} I_b \mathrm{d}t \quad (2)$$

Where: Q_b is the power battery capacity (Ah), t is the terminal moment.

2.3 Degradation model

Fuel cell system degradation is affected by operating conditions which can be classified into four categories: load variation, startup and shutdown, idling and high power loads.The empirical equation for the percentage drop is given below [11]:

$$D_{fc} = k_1 t_1 + k_2 n_1 + k_3 t_2 + k_4 t_3 \quad (3)$$

Where: D_{fc} is the percentage decline in fuel cell decline, t_1, n_1, t_2 and t_3 denote idle time, number of starts and stops, heavy load duration, and variable load burst time, respectively. k_1, k_2, k_3 and k_4 are the degradation coefficients for each category.

The power battery life model adopts the empirical model of battery capacity loss, the power battery in this paper is a simplified model, and the temperature is a constant value, only the battery capacity loss caused by the accumulated charge is considered, and the expression is as follows [12]:

$$\begin{cases} Q_{loss} = (\alpha SOC + \beta)\exp(\dfrac{-31700 + 163.3 I_c}{RT_b}) Q^{0.57} \\ \alpha = \begin{cases} 1287.6, SOC \le 0.45 \\ 1385.5, SOC > 0.45 \end{cases} \\ \beta = \begin{cases} 6356.3, SOC \le 0.45 \\ 4193.2, SOC > 0.45 \end{cases} \end{cases} \quad (4)$$

Where: Q_{loss} is the cell capacity loss, B is the pre-finger factor, E_a is the activation energy (J), R is the gas molar constant, T_b is the battery temperature (K), Q is the cumulative charge (C),α， β is a constant term, I_c is the discharge multiplier (1/h).

3. INTEGRATED CONTROL SYSTEM

In the ITS environment, FCHV obtains traffic environment information through Vehicle to Vehicle (V2V) and Vehicle to Infrastructure (V2I). The overall control framework is shown in Fig.3.

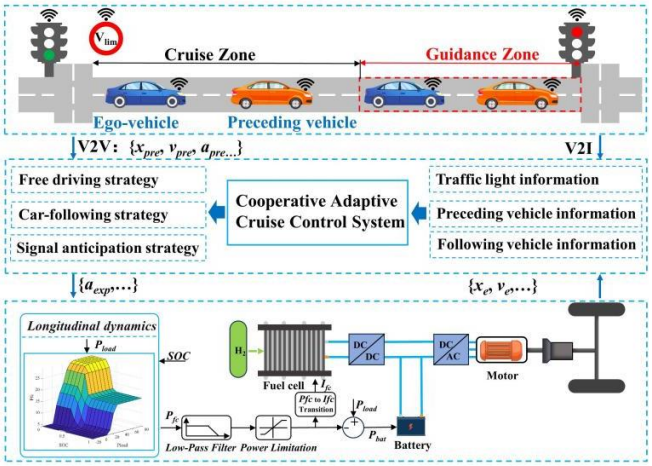

Fig. 3. Integrated CACC and EMS control system

3.1 Speed control model

The scenes encountered by the vehicle are mainly divided into three categories : free driving, car-following and signal guidance mode. Considering the control modes of CACC vehicles in different scenarios, the traditional Intelligent Driver Model (IDM) model is extended to establish acceleration algorithms under different control modes.

3.1.1 Free cruise

In free cruise scenario, the primary vehicle travels at a cruising speed that is not higher than the maximum speed limit of the current lane, and the formula for the cruising speed of the vehicle in the free scenario is as follows [11]:

$$a_{Fd} = \begin{cases} a\left|1 - (\dfrac{v_{exp}}{v_e(t)})^{\delta}\right| & v(t) \le v_{exp} \\ -b\left|1 - (\dfrac{v_e(t)}{v_{exp}})^{a\delta/b}\right| & v(t) > v_{exp} \end{cases} \quad (5)$$

Where: a_{Fd} is the vehicle cruising acceleration (m/s^2),a is the maximum acceleration (m/s^2), b is the maximum deceleration (m/s^2), v_{exp} is the cruising speed (m/s) set by the vehicle,δ is the model parameter.

3.1.2 Car-following

In the car-following scenario, the acceleration demand can be calculated in the CACC system based on the vehicle spacing and relative speed between the main vehicle and the vehicle in front of it, therefore, the vehicle adopts the following equations for following control [7]:

$$\begin{cases} a_{Cf}(t) = a_{pre}(t) + k_v \Delta v(t) + k_s(\Delta s(t) - s_{des}(t)) \\ \Delta v(t) = v_{pre}(t) - v_e(t) \\ \Delta s(t) = s_{pre}(t) - s_e(t) \end{cases} \quad (6)$$

The desired spacing is the following spacing set according to the headway time distance, and the desired spacing is set as considering the safe tracking distance for the vehicle deceleration capability:

$$s_{des}(t) = s_0 + v_e(t) T_h + L \quad (7)$$

Where: S_0 is the safety distance (5m), T_h is the head time distance (1.5s), and L is the length of the vehicle (m).

3.1.3 Signal guidance

Based on the variable expected distance model, considering the relative speed with the front vehicle, the cruise distance model is designed, such as Equation (9), to determine the switching threshold of the two cruise modes :

$$d_s = \begin{cases} s_{des} + r_{acc}\Delta v & \Delta v > 0 \\ s_{des} + r_{dec}\Delta v & \Delta v < 0 \end{cases} \quad (8)$$

Where: d_s is the cruise and follow cruise switching distance threshold (m), r_{acc} and r_{dec} is is the weighting coefficient.

When the remaining distance between the vehicle and the signal is equal to the length *D* of the signal guidance zone, the current information is used to comprehensively judge whether the vehicle can pass the signal intersection.

$$S_{sig} = \begin{cases} T_g v_e(t), T_g > 0 \\ T_r v_e(t), T_r > 0 \end{cases} \quad (9)$$

Where: S_{sig} is the predicted distance of the vehicle (m), T_g is the remaining time of the green light (s), T_r is the remaining time of the red light (s).

When the signal is green, if S_{sig} >D, it means the vehicle can pass the signalized intersection with the current speed, if S_{sig} ≤D, it means the vehicle cannot pass the signalized intersection.When the signal light is red, if S_{sig} <D, it indicates that the vehicle can pass the signalized intersection with the current speed cruise, if S_{sig}≥D, it indicates that the vehicle can not pass the signalized intersection with the current speed, and it needs to decelerate to a certain extent to pass the signalized intersection, and the deceleration to the signalized intersection is calculated by the equation (10) to determine whether it can be decelerated to the rear to maintain the speed to pass the signalized intersection, and if it can not pass the signalized intersection If it is not possible to pass the signalized intersection, the vehicle decelerates until it stops before the signalized intersection.

$$a_{reduce} = \frac{v_e - v_{min}}{3.6T_r} \quad (10)$$

3.2 Energy management strategy

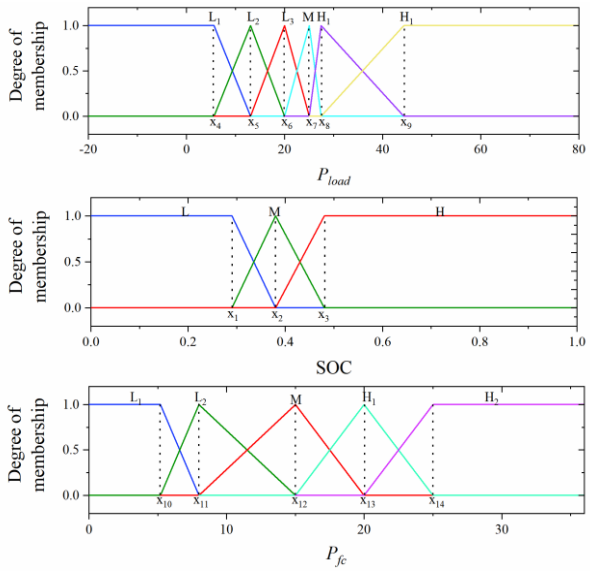

Fig. 4. Fuzzy logic control membership function

EMS is designed to coordinate the power distribution between fuel cells and power batteries. The object of this study is the extended-range FCHV, its EMS is divided into two stages : charge depletion and charge sustain. The EMS in this paper mainly focuses on the energy distribution in the charge sustain stage. This paper adopts EMS based on fuzzy logic control (FLC). The power battery SOC and the required power are selected as the input, and the membership function of the FLC is shown in Fig.4.

Durability is the current difficulty of fuel cell technology. Fuel cell durability is affected by system operating conditions, and dynamic power fluctuations, frequent system start-stop and low-power operation are detrimental to fuel cell health. The EMS of [2] is used to mitigate fuel cell power fluctuations by incorporating a low-pass filter. The established low-pass filter is as follows:

$$G(s) = \frac{2\pi f_c}{2\pi f_c + s} = \frac{1}{1+\tau s} \quad (11)$$

Where: f_c is the cutoff frequency , τ is a time constant.

4. RESULTS AND ANALYSIS

The overall performance of the vehicle is optimized by optimizing the main control parameters in the system. The multi-objective optimization problem related to the decision vector in this paper is defined as :

$$\min_{X=[k_v, k_s, \ldots]} J = [J_{FS}, J_{DC}, J_{FE}, J_{PD}] \quad (12)$$

Based on the CMOPSO algorithm, the multi-objective optimization of the control parameters under the integrated framework of CACC and EMS is carried out in the real road scene of urban multi-signal lights. Firstly, based on the Pareto method, multiple optimization objectives are processed to obtain the Pareto front. Then, the method based on traditional weighted sum is used as a comparison. It is compared with the original control strategy which is optimized and calibrated only under the WLTC standard working condition and not optimized under the actual road condition.

Since only one optimization result is usually required, in order to find a compromise solution that considers all targets, the following formulas are used to sort the particles in the Pareto optimal solution set at the same scale.

$$\min_{K \in PF} f(J(K)) = \min_{K \in PF} \sum_{i=1}^{4} \frac{J_i(K) - J_i^{min}}{J_i^{max} - J_i^{min}} \quad (13)$$

Where: J_i^{max} and J_i^{min} is the maximum and minimum values for each objective in the set of Pareto optimal solutions. The best compromise solution obtained based on this method is considered as the optimal solution in the Pareto frontier and is applied to the integrated CACC and EMS control framework proposed in this paper.

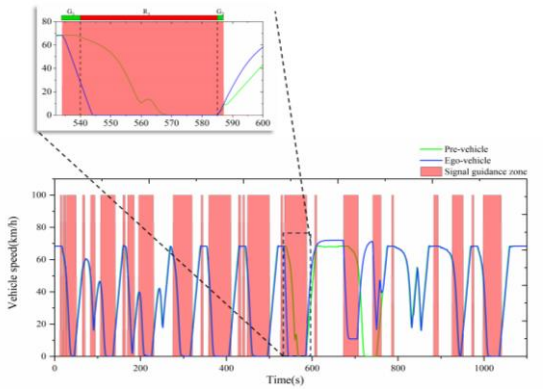

Fig. 5. Speed profile by the CACC strategy

Fig.5 shows that our proposed strategy ensures that the FCHV makes appropriate driving choices to follow the vehicle in front or slow down early. At 17 signalized intersections (585s), the vehicle decelerates early and idles at the red light when the Ego-vehicle is unable to safely pass through the intersection during the green light window. When waiting for the next green light to turn on, the free cruise scenario was triggered and the vehicle cruised at a set speed that did not exceed the road speed limit because there is no vehicle in the detection range in front of the vehicle to follow. When the vehicle cruises to the 19th intersection, the Ego-vehicle decelerates early, without coming to a complete stop, before passing through the intersection in the next green light window. As the Ego-vehicle passed through the intersection, the vehicle quickly and smoothly caught up with the vehicle in front of it until a safe following distance was reached. The results show that the Ego-vehicle can make appropriate driving choices based on real-time driving information in continuous signalized intersection scenarios.

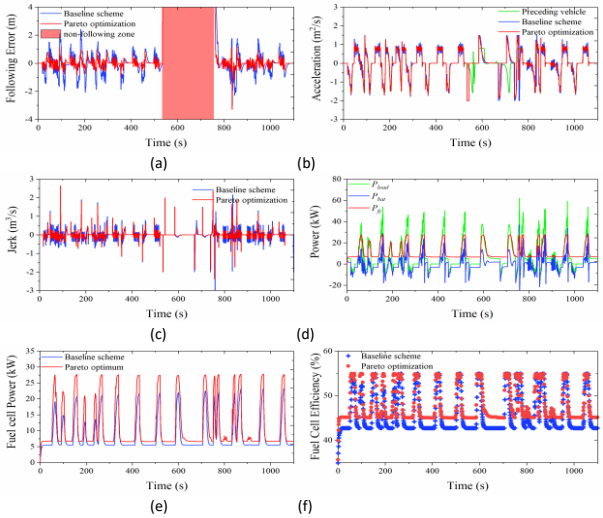

Fig. 6. Simulation results

Fig.6 (a) shows that the tracking error can be reduced after optimization, while the tracking error of the baseline strategy is slightly larger, which indicates that the optimized tracking condition is more stable. Fig.6 (b-c) shows the acceleration and jerk of the vehicle, which can be optimized to reduce the magnitude of the acceleration fluctuation of the vehicle and improve the driving comfort. Fig.6 (d) shows the results of the power allocation, and the EMS can satisfy the load demand while maintaining the stable output of fuel cell power, and after the low-pass filter adjustment, the high frequency part is provided by the power cell, which reduces the power fluctuation of the fuel cell and helps to alleviate the degradation of the fuel cell. Hydrogen consumption is saved by recovering energy from braking. Fig.6 (e-f) Comparison results of fuel cell outputs, demonstrating the improvement of fuel cell efficiency based on the Pareto method, suggesting that the longitudinal control and energy distribution of the vehicle can be effectively improved through the synergistic optimization.

Table 2 shows the performance of the benchmark, the Pareto-based method, and the weighted sum of the three methods for different objectives between the two methods in an urban roadway scenario. The results show that the Pareto-based method minimizes the average following error (58.1%), the average speed variation (1.2%), the equivalent hydrogen consumption cost (4.1%), and the combined power degradation cost (2.1%) with respect to the baseline method.Weighted-sum 2 focuses more on driving safety, which is the best among the five sets of results. While several other weightings tend to reduce driving safety. In the chaotic particle swarm algorithm, the weighted-sum based approach, with a single comprehensive objective function as the decision vector for deciding the direction of particle flight, is unable to weigh multiple objectives, which makes the optimization results easily deviate from the optimal solution as the dimension and scale of the search increases. Therefore, the Pareto-based approach can completely improve driving comfort, reduce equivalent hydrogen consumption, and extend power source lifespan.

Table 2 Comparison of Pareto and weighted-sum method

Objective index	J_{FS}(m)	J_{DC}(m/s^2)	J_{FE}($)	J_{PD}($)
Baselinescheme	0.635	0.474	1.789	0.333
Weighted-sum 1	0.176	0.475	1.751	0.335
Weighted-sum 2	**0.172**	0.479	1.777	0.331
Weighted-sum 3	0.188	0.474	1.752	0.329
Weighted-sum 4	0.179	0.473	1.790	0.336
Pareto method	0.266	**0.468**	**1.715**	**0.326**

5. CONCLUSIONS

In this paper, considering the uncertainty of driving conditions and the energy management of the powertrain, the integrated framework of CACC and EMS is established, and a parameter optimization method based on the Pareto method is proposed to optimize the integrated framework. Simulation results validate the effectiveness of the method, and the proposed optimization method achieves 58.1%, 1.2%, 4.1%, and 2.1% in terms of driving safety, comfort-equivalent hydrogen consumption cost, and power degradation cost, compared with the calibrated baseline strategy under WLTC conditions. Compared to the weighted sum based optimization approach, the adopted approach can overcome the uncertainty constraints of the weighting factors and find the best compromise solution. In future work, the vehicle speed prediction method under the grid-connected framework will be introduced to optimize the control parameters based on the predicted speed, focusing on the trade-off between the prediction step size and the real-time nature of the computational capability.

ACKNOWLEDGEMENT

This study is supported by the National Key R&D Program of China (2021YFB2501303). We sincerely appreciate this project for all the help it has provided to the completion of this manuscript.

DECLARATION OF INTEREST STATEMENT

The authors declare that they have no known competing financial interests or personal relationships that could have appeared to influence the work reported in this paper. All authors read and approved the final manuscript.

REFERENCE

[1] Y. Jia, Z. Nie, W. Wang, Y. Lian, J. M. Guerrero, and R. Outbib, "Eco-driving policy for connected and automated fuel cell hybrid vehicles platoon in dynamic traffic scenarios," *International Journal of Hydrogen Energy,* Article vol. 48, no. 49, pp. 18816-18834, Jun 8 2023.

[2] H.-B. Yuan, W.-J. Zou, S. Jung, and Y.-B. Kim, "Optimized rule-based energy management for a polymer electrolyte membrane fuel cell/battery hybrid power system using a genetic algorithm," *International Journal of Hydrogen Energy,* Article vol. 47, no. 12, pp. 7932-7948, Feb 8 2022.

[3] S. Changizian, P. Ahmadi, M. Raeesi, and N. Javani, "Performance optimization of hybrid hydrogen fuel cell-electric vehicles in real driving cycles," *International Journal of Hydrogen Energy,* Article vol. 45, no. 60, pp. 35180-35197, Dec 9 2020.

[4] Y. Zhang *et al.*, "An optimal control strategy design for plug-in hybrid electric vehicles based on internet of vehicles," *Energy,* Article vol. 228, Aug 1 2021.

[5] F. Zhang, X. Hu, R. Langari, and D. Cao, "Energy management strategies of connected HEVs and PHEVs: Recent progress and outlook," *Progress in Energy and Combustion Science,* Review vol. 73, pp. 235-256, Jul 2019.

[6] K. C. Dey *et al.*, "A review of communication, driver characteristics, and controls aspects of cooperative adaptive cruise control (CACC)," *IEEE Transactions on Intelligent Transportation Systems,* Article vol. 17, no. 2, pp. 491-509, Feb 2016.

[7] L. Zhu, F. Tao, Z. Fu, H. Sun, B. Ji, and Q. Chen, "Multiobjective optimization of safety, comfort, fuel economy, and power sources durability for FCHEV in car-following scenarios," *IEEE Transactions on Transportation Electrification,* Article vol. 9, no. 1, pp. 1797-1808, Mar 2023.

[8] Z. Nie, Y. Jia, W. Wang, Z. Chen, and R. Outbib, "Co-optimization of speed planning and energy management for intelligent fuel cell hybrid vehicle considering complex traffic conditions," *Energy,* Article vol. 247, May 15 2022.

[9] C. Hong-jun, Z. Min-qing, X. Jiang-ke, and S. Chang-bai, "Study on ACC vehicle control mode under cooperative vehicle infrastructure guidance strategy for signalized intersection,'' *Journal of Highway and Transportation Research and Development,* vol. 36, no. 06, pp. 86-93, 2019.

[10]Z. Chen, S. Wu, S. Shen, Y. Liu, F. Guo, and Y. Zhang, "Co-optimization of velocity planning and energy management for autonomous plug-in hybrid electric vehicles in urban driving scenarios," *Energy,* Article vol. 263, Jan 15 2023.

[11]Z. Hu *et al.*, "Multi-objective energy management optimization and parameter sizing for proton exchange membrane hybrid fuel cell vehicles," *Energy Conversion and Management,* Article vol. 129, pp. 108-121, Dec 1 2016.

[12]L. Tang, G. Rizzoni, and S. Onori, "Energy management strategy for HEVs including battery life optimization," *IEEE Transactions on Transportation Electrification,* Article vol. 1, no. 3, pp. 211-222, Oct 2015.